Formation of Dimer Radical Anions of Aromatic Acetylenes during Pulse Radiolysis and γ-Radiolysis

Tetsuro Majima,*,† Sachiko Tojo, and Setsuo Takamuku

The Institute of Scientific and Industrial Research, Osaka University, Mihogaoka 8-1, Ibaraki, Osaka 567, Japan

Received: September 30, 1996; In Final Form: November 23, 1996[⊗]

Dimerization of the radical anions of aromatic acetylenes ($A^{\bullet-}$) such as diphenylacetylene and its derivatives with substituents on the benzene ring (**1**$^{\bullet-}$), 1,4-diphenyl-1,3-butadiyne (**2**$^{\bullet-}$), and intramolecular dimer model compounds having two diphenylacetylene chromophores linked by several methylene chains (**3**$^{\bullet-}$) has been studied with pulse radiolysis of A in solutions at room temperature and γ-radiolysis in rigid matrices of A at 77 K. The transient absorptions of $A^{\bullet-}$ decayed with the formation of new bands assignable to the dimer radical anions of $A^{\bullet-}$ and A. Because the decay and formation depend on the concentration of A, the bimolecular rate constants of $k_b = 7.3 \times 10^6$ to 6.6×10^7 M^{-1} s^{-1} were estimated for the intermolecular dimerization at room temperature. The spectral changes were also observed upon warming of 77 K rigid matrices of $A^{\bullet-}$. It is suggested that $A^{\bullet-}$ dimerizes with A through the formation of one C−C bond between two sp carbons, giving σ-type dimer radical anions (σ-$A_2^{\bullet-}$) with a diene-type structure. Absorption spectra similar to those of **1**$^{\bullet-}$ were initially observed in **3**$^{\bullet-}$ generated by the radiolyses but changed to those assignable to the intramolecular dimer radical anions similar to σ-**1**$_2^{\bullet-}$. The yield of the dimer radical anions of **3**$^{\bullet-}$ with a tetramethylene chain was the largest among the dimer radical anions with several methylene chains.

Introduction

Whether or not the radical anion of aromatic hydrocarbons ($ArH^{\bullet-}$) is stabilized by a charge resonance (CR) π-interaction with ArH, giving the dimer radical anion, $(ArH)_2^{\bullet-}$, has been examined. Although much effort has been concentrated on detecting $(ArH)_2^{\bullet-}$ with a sandwich structure between two aromatic groups of $ArH^{\bullet-}$ and ArH, the formation of $(ArH)_2^{\bullet-}$ has not been observed.[1−10] As an exceptional case, the dimer radical anion of anthracene has been formed from the cleavage of a $4\pi+4\pi$ anthracene photodimer radical anion in a rigid matrix at 77 K.[3a] Radical anions of several olefins with electron-withdrawing substituents such as fumaronitrile, maleic anhydride, and acrylonitrile have been observed to dimerize to give the dimer radical anions which are assumed to have a broad absorption band in the 800−1700 nm range.[2c]

On the other hand, the ArH radical cation ($ArH^{\bullet+}$) is well-known to dimerize with ArH to give associated (π-type) and/or bonded (σ-type) dimer radical cations, $(ArH)_2^{\bullet+}$, which are important ionic intermediates in radiation chemistry, photochemistry, and electrochemistry.[11−22] For example, we have reported that the *trans*-stilbene radical cation (*t*-$St^{\bullet+}$) dimerizes with *t*-St to give a π-type St dimer radical cation, π-$St_2^{\bullet+}$ with a face-to-face structure, which converts to a σ-type $St_2^{\bullet+}$ with a single bond between two olefinic carbons based on the absorption spectral change during pulse radiolysis.[22a]

In contrast to $St^{\bullet+}$, no dimerization of $St^{\bullet-}$ with St has been observed. It has been reported that $St^{\bullet-}$ reacts with $St^{\bullet-}$ to give the stilbene dianion (St^{2-}) and St via disproportionation[6,7] at higher concentrations of $St^{\bullet-}$. On the other hand, the diphenylacetylene radical anion (**1a**$^{\bullet-}$) reacts with **1a**$^{\bullet-}$ to give the **1a** dimer dianion, (**1a**)$_2^{2-}$ with an absorption peak at λ_{max} = 470 nm ($\epsilon_{470} = 9.0 \times 10^3$ and 1.1×10^4 M^{-1} cm^{-1} in tetrahydrofuran (THF)[7] and hexamethylphosphoric triamide (HMPA),[8] respectively) at higher concentrations of **1a**$^{\bullet-}$, [**1a**$^{\bullet-}$] = (2.6−7.3) $\times$ 10^{-2} and 3.5 $\times$ 10^{-3} M in THF[7] and HMPA,[8] respectively. The structure of (**1a**)$_2^{2-}$ is assumed to be the 1,2,3,4-tetraphenylbut-1,3-ene-1,4-diyl dianion (PhC^-═CPh−CPh−C^-═Ph) with the formation of one C−C bond between two sp carbons.[7,8]

We report here that the aromatic acetylene radical anions ($A^{\bullet-}$) such as **1a**$^{\bullet-}$, 4-methyl-(**1b**$^{\bullet-}$), 4-phenyl- (**1c**$^{\bullet-}$), 4-nitro-(**1d**$^{\bullet-}$), 4-methoxy- (**1e**$^{\bullet-}$), and the 4-fluorodiphenylacetylene (**1f**$^{\bullet-}$) radical anions, 2,3,4,5,6-pentaphenyldiphenylacetylene radical anion (**1g**$^{\bullet-}$), and 1,4-diphenyl-1,3-butadiyne radical anion (**2**$^{\bullet-}$) dimerize with A to form the dimer radical anion ($A_2^{\bullet-}$). We also observed that the intramolecular dimerization

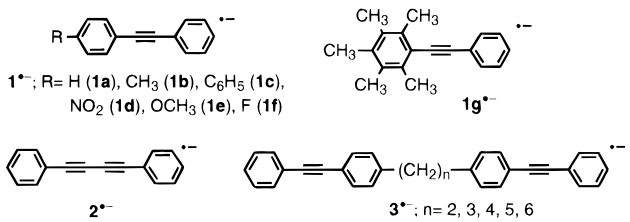

occurs in 1,ω-di-(4-(diphenylacetylenyl))ethane (**3**$^{\bullet-}$ (n = 2)), -propane (**3**$^{\bullet-}$ (n = 3)), -butane (**3**$^{\bullet-}$ (n = 4)), -pentane (**3**$^{\bullet-}$ (n = 5)), and -hexane (**3**$^{\bullet-}$ (n = 6)) radical anions to give the intramolecular dimer radical anions of diphenylacetylene chromophores based on absorption spectral measurements using the γ-radiolysis of 2-methyltetrahydrofuran (MTHF) rigid matrices at 77 K and the pulse radiolysis of HMPA and *N*,*N*-dimethylformamide (DMF) solutions at room temperature.

Experimental Section

General. Pulse radiolyses were performed, as described previously,[22a] using an electron pulse (28 MeV, 8 ns, 0.7 kGy per pulse) from a linear accelerator at Osaka University. γ-Radiolyses were carried out using a ^{60}Co γ source (dose, 2.6

† Tel: Japan+6-879-8496. Fax: Japan+6-875-4156. E-mail:majima@sanken.osaka-u.ac.jp.

⊗ Abstract published in *Advance ACS Abstracts,* January 1, 1997.

S1089-5639(96)02999-4 CCC: $14.00

$\times 10^2$ to 1.0×10^3 Gy).[22a] Optical absorption spectra were taken by a spectrophotometer and a multichannel photodetector.

Hexamethylphosphoric triamide (HMPA) or *N*,*N*-dimethylformamide (DMF) solutions containing **1**−**3** with 3.0×10^{-3} to 4.0×10^{-2} M were used for the pulse radiolyses; 2-methyltetrahydrofuran (MTHF) solutions containing **1**−**3** with 3.0×10^{-3} to 5.0×10^{-2} M were used for the γ-radiolyses. The solutions were prepared freshly in 1 cm × 1 cm rectangular Suprasil cells for the pulse radiolyses and in 1.5-mm-thick Suprasil cells for UV−vis absorption measurements at 77 K before irradiation and were degassed by freeze−pump−thaw cycles.

Materials. **1a** and **2** were purchased from Aldrich and Tokyo Kasei and purified by means of recrystallization from ethanol before use. The other acetylenes (**1b**−**1f** and **3** ($n = 2-6$)) were synthesized from reactions of phenylacetylenylcopper (0.02 mol) with the corresponding substituted iodobenzene (0.02 mol) and 1,ω-di(4-iodophenyl)alkane, respectively, in pyridine according to literature procedures[23] and purified by means of column chromatography on silica gel and recrystallization from ethanol before use (Supporting Information). Analyses of the purified **1**−**3** by GC showed purities higher than 99.5%. Other chemicals were purchased from Tokyo Kasei and purified by distillation or recrystallization prior to use.

2-Methyltetrahydrofuran (MTHF), hexamethylphosphoric triamide (HMPA), or *N*,*N*-dimethylformamide (DMF) used as a solvent were fractionally distilled.

Results and Discussion

Formation of Dimer Radical Anion, $(\mathbf{1a})_2^{\bullet-}$. It is well established that the radical anions of aromatic hydrocarbons (ArH) are generated during the γ-radiolysis of ArH in MTHF rigid matrices at 77 K and the pulse radiolysis of HMPA and DMF solutions at room temperature.[1−10] $G(e^-) = 2.3$ has been reported for the G value of the formation of the solvated electrons in HMPA,[4] where the G value is defined as the number of the electrons produced per 100 eV of radiation energy absorbed by a sample solution. The same G value is used for the formation of $ArH^{\bullet-}$ as the maximum G value, because it is assumed that all the electrons convert into $ArH^{\bullet-}$ with the bimolecular rate constant of the electron attachment, $10^{11}-10^{12}$ M^{-1} s^{-1} in THF.[1,3] The transient absorption spectrum with $\lambda_{max} = 450$ and >840 nm was immediately observed after the electron pulse during the pulse radiolysis of **1a** with 5.0×10^{-3} to 4.0×10^{-2} M in degassed HMPA solutions at room temperature (Figure 1a). The bands at $\lambda_{max} = 450$ nm ($\epsilon_{450} = 2.7 \times 10^4$, 5.6×10^4, and $(5.4-5.6) \times 10^4$ M^{-1} cm^{-1} in THF, MTHF, and HMPA, respectively) and $\lambda_{max} = 860$ nm ($\epsilon_{860} = 1.7 \times 10^4$ M^{-1} cm^{-1} in HMPA) have been already assigned to $\mathbf{1a}^{\bullet-}$ generated during the pulse radiolysis at room temperature,[3b,4,9a] the γ-radiolysis in an MTHF rigid matrix at 77 K,[3c] and during the reduction by sodium metal in THF and HMPA.[7,8] Similar absorption spectra were observed during the pulse radiolysis in DMF (Figure 1b) and during the γ-radiolysis in an MTHF rigid matrix at 77 K (Figure 2). The concentration of $\mathbf{1a}^{\bullet-}$ generated immediately after irradiation with an electron pulse was calculated to be $[\mathbf{1a}^{\bullet-}]_0 = 8.3 \times 10^{-5}$ M from the transient optical density at 450 nm ($\Delta OD_{450} = 1.8$) observed, $\epsilon_{450} = 5.4 \times 10^4$ M^{-1} cm^{-1} reported for $\mathbf{1a}^{\bullet-}$ in HMPA[8,24] and the optical path length of $l = 0.4$ cm.

The transient absorption of $\mathbf{1a}^{\bullet-}$ decayed on a time scale of a few microseconds with the formation of a band at $\lambda_{max} = 500$ nm with isosbestic points at 470 and 630 nm at room temperature. The pseudo-first-order rate constants of the decay of the 450 nm band and the formation of the 500 nm band,

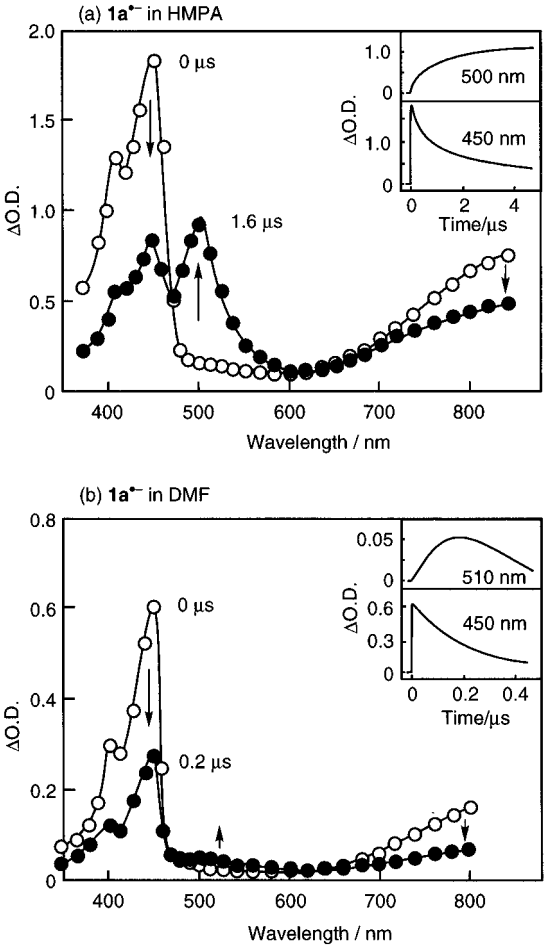

Figure 1. Transient absorption spectral changes during the pulse radiolysis of **1a** at 1.0×10^{-2} M in degassed HMPA (a) and DMF (b) solutions at room temperature. Insets: time profiles of the transient absorptions at λ_{max} which are denoted in the figure.

k_d^{450} and k_f^{500}, respectively, were calculated from the first-order rate equation. The decay rates were similar in magnitude to the formation rate within the experimental error. For example, $k_d^{450} = 1.0 \times 10^6$ and $k_f^{500} = 1.3 \times 10^6$ s^{-1} at $[\mathbf{1a}] = 10^{-2}$ M. It is found that k_d^{450} and k_f^{500} increase with increasing [**1a**]. This suggests that $\mathbf{1a}^{\bullet-}$ dimerizes with **1a** to give the dimer radical anion, $(\mathbf{1a})_2^{\bullet-}$, with the formation of the 500 nm band.

A similar absorption spectral change of $\mathbf{1a}^{\bullet-}$ was observed in the MTHF rigid matrix at 77 K after the γ-radiolysis of **1a** (Figure 2). The absorption bands of $\mathbf{1a}^{\bullet-}$ at $\lambda_{max} = 450$ and >800 nm disappeared upon warming below 100 K, while a 500 nm band appeared. This result suggests that $\mathbf{1a}^{\bullet-}$ dimerizes with **1a** to $(\mathbf{1a})_2^{\bullet-}$ with the 500 nm band.

It is well-known that $ArH^{\bullet-}$ does not dimerize with ArH,[1−10] except for the π-type anthracene dimer radical anion in a rigid matrix at 77 K[3a] and several olefin dimer radical anions with strong electron-withdrawing substituents such as fumaronitrile, maleic anhydride, acrylic esters, methyl vinyl ketone, acrolein, and acrylonitrile dimer radical anions in solution at room temperature and rigid matrices at 77 K.[2] The formation and reactivities of $\mathbf{1a}^{\bullet-}$ have been studied during electrolysis, the reduction by sodium metal, photolysis, and radiolysis.[3b,3c,7,8,25,26] No dimerization of $\mathbf{1a}^{\bullet-}$ with **1a** has been reported. On the other hand, the experimental results indicate that $\mathbf{1a}^{\bullet-}$ dimerizes with **1a** to give $(\mathbf{1a})_2^{\bullet-}$ along with the 500 nm band (eq 1).

$$\mathbf{1a}^{\bullet-} + \mathbf{1a} \rightarrow (\mathbf{1a})_2^{\bullet-} \quad (1)$$

The bimolecular rate constant of the dimerization (k_b) was calculated from the linear plots of the observed rate constants

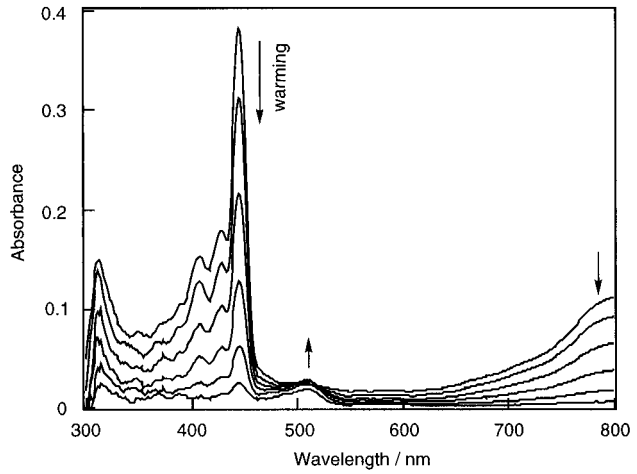

Figure 2. Absorption spectral changes of $\mathbf{1a}^{\bullet-}$ upon warming below 100 K after γ-radiolysis of MTHF rigid matrix containing **1a** at 5.0×10^{-3} M at 77 K.

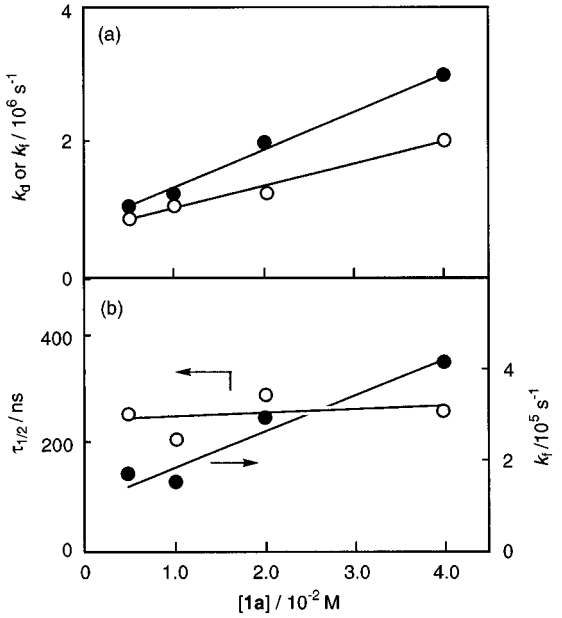

Figure 3. Plots of the pseudo-first-order rate constant, k_d and k_f calculated from the decay of transient absorptions at 450 (○) and the formation at 500 nm (●) in HMPA, and plots of the half-lifetime of the decay of the 450 band (○) and k_f of the formation of the 510 nm band (●) in DMF vs [**1a**] during the pulse radiolysis of **1a** in degassed HMPA (a) and DMF (b) solutions at room temperature.

(pseudo-first-order rate constants) of the decay of the 450 and 800 nm bands and the formation of the 500 nm band (k_d^{450} and k_f^{500}, respectively) vs [**1a**] (Figure 3). The value of $k_b = 6.6 \times 10^7$ M^{-1} s^{-1} was obtained from the plot of k_f^{500} vs [**1a**], while smaller values of $k_b = 3.8 \times 10^7$ M^{-1} s^{-1} were from the plot of k_d^{450}. The differences are probably due to the overlapping absorption bands of $\mathbf{1a}^{\bullet-}$ and $(\mathbf{1a})_2^{\bullet-}$ in the wavelength range.

Both a π-type sandwich structure and a σ- or diene-type structure are most likely for $(\mathbf{1a})_2^{\bullet-}$ with a band at $\lambda_{max} = 500$ nm. The 500 nm band is assigned to σ-$(\mathbf{1a})_2^{\bullet-}$ with a C−C bond between sp carbons of $\mathbf{1a}^{\bullet-}$ and $(\mathbf{1a})_2^{\bullet-}$ (Scheme 1), since it is similar to the 470 nm band of dianion $(\mathbf{1a})_2^{2-}$, $PhC^-{=}CPhCPh{=}C^-Ph$, formed from the addition reaction of two $\mathbf{1a}^{\bullet-}$s.[7,8] Since *cis*-$St^{\bullet-}$ has an absorption band at 515 nm, a cyclobutadiene-type structure with two C−C bonds between the sp carbons formed from the $2\pi+2\pi$ cycloaddition would be assumed for $(\mathbf{1a})_2^{\bullet-}$ with no conjugation of the two *cis*-St chromophores. Such a structure would not be stable, since a planar structure is expected to be the most stable for 1,2,3,4-

SCHEME 1

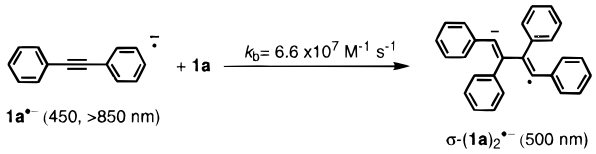

tetraphenylcyclobutadiene and the radical anion. If $(\mathbf{1a})_2^{\bullet-}$ had a π-type sandwich structure, a charge resonance (CR) absorption band in the 800−1700 nm range would be expected. Decay of the transient absorption in the 800 nm range suggests no formation of a strong CR absorption band due to $(\mathbf{1a})_2^{\bullet-}$, although a CR band would be expected at much longer wavelengths. This result does not suggest the π-type sandwich structure for $(\mathbf{1a})_2^{\bullet-}$. Consequently, it is suggested that the formation of σ-$(\mathbf{1a})_2^{\bullet-}$ is caused by the dimerization of $\mathbf{1a}^{\bullet-}$ and **1a**.

Effects of Substituents on Formation of $(\mathbf{1a})_2^{\bullet-}$. To determine the effects of substituents on the formation of $(\mathbf{1a})_2^{\bullet-}$, the dimerization of radical anions of monosubstituted diphenylacetylene with methyl, phenyl, nitro, methoxyl, and fluoro groups at the 4-position on one phenyl ring and 2,3,4,5,6-pentamethyldiphenylacetylene has been examined. The transient absorption spectra of $\mathbf{1b}^{\bullet-}$−$\mathbf{1g}^{\bullet-}$ with $\lambda_{max} = 440-500$ and >840 nm were immediately observed after the electron pulse during the pulse radiolysis of **1b**−**1g** with 3.0×10^{-3} to 2.5×10^{-2} M in degassed HMPA solutions at room temperature (Table 1 and Supporting Information). HMPA is a useful solvent to obtain sufficient solubilities of compounds and to stabilize the radical anions generated during the pulse radiolysis. The values of $\lambda_{max} = 440-450$ nm for $\mathbf{1b}^{\bullet-}$−$\mathbf{1f}^{\bullet-}$ are similar to $\lambda_{max} = 450$ nm for $\mathbf{1a}^{\bullet-}$, while $\lambda_{max} = 500$ nm for $\mathbf{1c}^{\bullet-}$ shifted to a longer wavelength compared with $\mathbf{1a}^{\bullet-}$ because $\mathbf{1c}^{\bullet-}$ has a biphenyl chromophore. It has been reported that the solvated electrons are attached to ArH with the rate constant of $10^{10}-10^{12}$ M^{-1} s^{-1} depending on the ArH and solvent, and it is assumed that all the solvated electrons convert to $ArH^{\bullet-}$.[1,3] Therefore, the concentrations of $\mathbf{1b}^{\bullet-}$−$\mathbf{1f}^{\bullet-}$ are reasonably assumed to be $[\mathbf{1b}^{\bullet-}]_0-[\mathbf{1g}^{\bullet-}]_0 = [\mathbf{1a}^{\bullet-}]_0 = 8.3 \times 10^{-5}$ M in HMPA as the maximum values immediately after irradiation with an electron pulse (8 ns). The ϵ_{max} values were calculated from ΔOD_0 at λ_{max} for $\mathbf{1}^{\bullet-}$, $[\mathbf{1}^{\bullet-}]_0 = 8.3 \times 10^{-5}$ M, and $l = 0.4$ cm (Table 1).

The transient absorption of $\mathbf{1b}^{\bullet-}$−$\mathbf{1g}^{\bullet-}$ decayed with the formation of a band in the range 500−550 nm with isobestic points in the ranges of 460−510 and 560−650 nm (Supporting Information). The decay rate of the band at 440−500 nm and the formation rate of the band at $\lambda_{max} = 500-550$ nm increased with increasing [**1b**]−[**1g**]. The 500−550 nm bands are assigned to the dimer radical anions of $\mathbf{1b}^{\bullet-}$−$\mathbf{1g}^{\bullet-}$ and **1b**−**1g**, σ-$(\mathbf{1b})_2^{\bullet-}$−$(\mathbf{1g})_2^{\bullet-}$, similar to that of σ-$(\mathbf{1a})_2^{\bullet-}$ (eq 1 and Scheme 1). Plots of the observed rate constants (pseudo-first-order rate constants, k_f) of the formation of the 500−550 nm band vs [**1b**]−[**1g**] were linear and gave the bimolecular rate constant, $k_b = 7.3 \times 10^6$ to 5.7×10^7 M^{-1} s^{-1} (Supporting Information), similar to that of $\mathbf{1a}^{\bullet-}$ as shown in Figure 3. The k_b values listed in Table 1 were of same order of magnitude for $\mathbf{1a}^{\bullet-}$−$\mathbf{1c}^{\bullet-}$ ($k_b = (4.1-6.6) \times 10^7$ M^{-1} s^{-1}), while those for $\mathbf{1d}^{\bullet-}$−$\mathbf{1g}^{\bullet-}$ were smaller ($k_b = 7.3 \times 10^6$ to 1.7×10^7 M^{-1} s^{-1}). The experimental results do not suggest a π-type sandwich structure for $\mathbf{1}_2^{\bullet-}$.

ΔOD_{max} values of $\mathbf{1a}^{\bullet-}$−$\mathbf{1c}^{\bullet-}$, $\mathbf{1e}^{\bullet-}$ and $\mathbf{1f}^{\bullet-}$ immediately after an electron pulse (at 0 μs) were in the range of 1.4−1.8 in HMPA, while the $\Delta OD_{max} = 0.95$ and 3.9 of $\mathbf{1d}^{\bullet-}$ and $\mathbf{1g}^{\bullet-}$, respectively, were smaller and larger than the $\Delta OD_{max} = 1.8$

TABLE 1: Intermolecular Dimerizations of A$^{\bullet-}$ and A (A = 1 and 2)[a]

		λ_{max}/nm		ΔOD_{max}					
$A^{\bullet-}$	substituents	$A^{\bullet-}$	$A_2^{\bullet-}$	$A^{\bullet-}$	$A_2^{\bullet-}$	$[A_2^{\bullet-}]_{max}/[A^{\bullet-}]_0$	$\epsilon_{max}/M^{-1}\,cm^{-1}$ of $A^{\bullet-}$	$k_b/M^{-1}\,s^{-1}$	solvent
1a$^{\bullet-}$	4-H	450	500	1.8	1.0	0.56	5.4×10^4 [b]	6.6×10^7	HMPA
1b$^{\bullet-}$	4-CH_3	450	510	1.4	0.90	0.66	4.1×10^4	5.7×10^7	HMPA
1c$^{\bullet-}$	4-C_6H_5	500	550	1.6	1.2	0.77	4.7×10^4	4.1×10^7	HMPA
1d$^{\bullet-}$	4-NO_2	440	490	0.95	0.09	0.10	2.7×10^4	9.0×10^6	HMPA
1e$^{\bullet-}$	4-OCH_3	440	500	1.7	0.15	0.09	5.2×10^4	1.0×10^7	HMPA
1f$^{\bullet-}$	4-F	440	500	1.8	0.25	0.15	5.4×10^4	1.7×10^7	HMPA
1g$^{\bullet-}$	$(CH_3)_5$	450	540	3.9	0.25	0.06	1.2×10^5	7.3×10^6	HMPA
1a$^{\bullet-}$	4-H	450	510	0.61	0.05	0.09	5.4×10^4 [c]	8.0×10^6	DMF
2$^{\bullet-}$	H	480	560	1.0	0.10	0.10	8.9×10^4	8.2×10^6	DMF

[a] $[A_2^{\bullet-}]_{max}/[A^{\bullet-}]_0 = (\Delta OD_{max}$ at λ_{max} for $A_2^{\bullet-})/(\Delta OD_0$ at λ_{max} for $A^{\bullet-})$. The ϵ_{max} values were calculated from ΔOD_0 at λ_{max} for $A^{\bullet-}$, $\epsilon_{max} = 5.4 \times 10^4\ M^{-1}\ cm^{-1}$ for **1a**$^{\bullet-}$,[8] $l = 0.4$ cm, and $[\mathbf{1}^{\bullet-}]_0 = 8.3 \times 10^{-5}$ M in HMPA, while ϵ_{480} for **2**$^{\bullet-}$ was calculated from $\epsilon_{450} = 5.4 \times 10^4\ M^{-1}\ cm^{-1}$ for **1a**$^{\bullet-}$, $l = 0.4$ cm, and $[\mathbf{1a}^{\bullet-}]_0 = 2.8 \times 10^{-5}$ M in DMF.[27] The bimolecular rate constant (k_b) of the dimerization of $A^{\bullet-}$ and A was calculated from the linear plot of k_f for the formation $A_2^{\bullet-}$ of vs [A]. [b] References 8 and 24. [c] References 24 and 27.

of **1a**$^{\bullet-}$ (Table 1). Because $[\mathbf{1}^{\bullet-}]_0 = 8.3 \times 10^{-5}$ M is approximately equivalent for **1a**$^{\bullet-}$−**1g**$^{\bullet-}$, ϵ_{max} values were calculated from ΔOD_{max} and $l = 0.4$ cm. The characteristics of the ϵ_{max} values of **1a**$^{\bullet-}$−**1g**$^{\bullet-}$ are the smaller and larger values of **1d**$^{\bullet-}$ and **1g**$^{\bullet-}$, respectively. Only strong electronic substituents on one benzene ring such as 4-nitro and 2,3,4,5,6-pentamethyl groups influence on ϵ_{max}. The $\Delta OD_{max} = 0.9$ and 1.2 of $(\mathbf{1b})_2^{\bullet-}$ and $(\mathbf{1c})_2^{\bullet-}$, respectively, were similar to the $\Delta OD_{max} = 1.0$ of $(\mathbf{1a})_2^{\bullet-}$, while the $\Delta OD_{max} = 0.09-0.25$ of $(\mathbf{1d})_2^{\bullet-}-(\mathbf{1g})_2^{-}$ were much smaller. The differences of ΔOD_{max} for **1**$^{\bullet-}$ are within a factor of 3, while those for $\mathbf{1}_2^{\bullet-}$ are within a factor of 10. The order of the ϵ_{max} of $\mathbf{1}_2^{\bullet-}$ may be expected to be the same as that of **1**$^{\bullet-}$. If the yield of $\mathbf{1}_2^{\bullet-}$ would be similar to that of **1**$^{\bullet-}$, the ratio of the ΔOD_{max} of $\mathbf{1}_2^{\bullet-}$ to the ΔOD_{max} of **1**$^{\bullet-}$ could be constant. However, the ratio was not constant (Table 1). They were of the same order of magnitude for **1a**$^{\bullet-}$−**1c**$^{\bullet-}$ (0.56−0.77), while those for **1d**$^{\bullet-}$−**1g**$^{\bullet-}$ were much smaller (0.06−0.15). The order of the ratio is similar to that of k_b. The k_b values for **1a**$^{\bullet-}$−**1c**$^{\bullet-}$ are larger than those for **1d**$^{\bullet-}$−**1g**$^{\bullet-}$.

It is summarized that the larger k_b leads to a higher yield of $\mathbf{1}_2^{\bullet-}$ and that the k_b and yields of $(\mathbf{1a})_2^{\bullet-}-(\mathbf{1c})_2^{\bullet-}$ with weak electronic substituents such as 4-methyl and 4-phenyl groups are comparable and those of $(\mathbf{1d})_2^{\bullet-}-(\mathbf{1g})_2^{\bullet-}$ with strong electronic substituents such as 4-nitro, 4-methoxyl, 4-fluoro, and 2,3,4,5,6-pentamethyl groups are much smaller. In other words, the dimerization of **1**$^{\bullet-}$ and **1** is not accelerated by π-interaction between **1**$^{\bullet-}$ and **1** but inhibited by steric and electronic effects of the substituents (**1b**$^{\bullet-}$−**1g**$^{\bullet-}$). The results may be attributed to heterogeneous distributions of a negative charge and an unpaired electron in **1d**$^{\bullet-}$−**1g**$^{\bullet-}$ and of π-electrons in **1d**−**1g**, and therefore, a higher barrier to a C−C bond formation between two sp carbons.

Solvent Effect on Formation of $(\mathbf{1a})_2^{\bullet-}$. Pulse radiolyses of **1a** in DMF and MTHF at room temperature were carried out to determine the solvent effect on the formation $(\mathbf{1a})_2^{\bullet-}$. The spectral change of **1a**$^{\bullet-}$ observed in DMF was similar to that in HMPA. The band of **1a**$^{\bullet-}$ at $\lambda_{max} = 450$ and >800 nm decayed with the formation of a band at $\lambda_{max} = 510$ nm assigned to $(\mathbf{1a})_2^{\bullet-}$ (Figure 1b). On the other hand, the band of **1a**$^{\bullet-}$ at $\lambda_{max} = 450$ nm decayed without any band formation in MTHF. Values of $\Delta OD_{max} = 0.61$ and 0.57 at $\lambda_{max} = 450$ nm for **1a**$^{\bullet-}$ in DMF and MTHF, respectively, were smaller than $\Delta OD_{max} = 1.8$ in HMPA. Because the $\epsilon_{450} = 5.4 \times 10^4\ M^{-1}\ cm^{-1}$ of **1a**$^{\bullet-}$ is the same in DMF, MTHF, and HMPA, $[\mathbf{1a}^{\bullet-}]_0 = 2.8 \times 10^{-5}$ and 2.6×10^{-5} M in DMF and MTHF, respectively, are calculated to be approximately one-third of $[\mathbf{1a}^{\bullet-}]_0 = 8.3 \times 10^{-5}$ M in HMPA. This is attributed to differences in $G(e^-)$ and $G(\mathbf{1a}^{\bullet-})$ in the solvents. The values of $G(e^-) = 0.8$ and 0.7 in DMF and MTHF, respectively, are estimated from $G(e^-) = 2.3$ in HMPA.[4,27]

If the yield of $(\mathbf{1a})_2^{\bullet-}$ would be the same in DMF and HMPA, it should be expected that the ratio of the ΔOD_{max} of $(\mathbf{1a})_2^{\bullet-}$ to the ΔOD_{max} of **1a**$^{\bullet-}$, equal to the ratio of $[(\mathbf{1a})_2^{\bullet-}]_{max}$ to $[\mathbf{1a}^{\bullet-}]_{max} = [\mathbf{1a}^{\bullet-}]_0$, would be the same in DMF and HMPA, and that the ratio of the ΔOD_{max} for **1a**$^{\bullet-}$ in DMF to that in HMPA should be similar to the ratio of the ΔOD_{max} for $(\mathbf{1a})_2^{\bullet-}$ in DMF to that in HMPA. However, the ratio $[(\mathbf{1a})_2^{\bullet-}]_{max}/[\mathbf{1a}^{\bullet-}]_0 = 0.09$ in DMF was smaller than 0.56 in HMPA (Table 1). The ratio of ΔOD_{max} at $\lambda_{max} = 450$ nm for **1a**$^{\bullet-}$ was 1:3 in DMF and in HMPA, while that of ΔOD_{max} at $\lambda_{max} = 500-510$ nm for $(\mathbf{1a})_2^{\bullet-}$ in DMF and in HMPA was 1:20. The results indicate that the yield of $(\mathbf{1a})_2^{\bullet-}$ is much lower in DMF than in HMPA.

Kinetic analyses of the time profiles of ΔOD_{max} of $(\mathbf{1a})_2^{\bullet-}$ in DMF were performed, although they included large errors because of the small values of ΔOD_{max}. The formation of the 510 nm band of $(\mathbf{1a})_2^{\bullet-}$ was analyzed by the pseudo-first-order rate equation with k_f^{510} which increased slightly with increasing [**1a**]. On the other hand, the decay profile of 450 nm band of **1a**$^{\bullet-}$ was almost constant with the half-lifetime of $\tau_{1/2} = 250$ ns in the range of $[\mathbf{1a}] = 5.0 \times 10^{-3}$ to 4.0×10^{-2} M. The bimolecular rate constant of $k_b = 8.2 \times 10^6\ M^{-1}\ s^{-1}$, estimated from the relation of k_f^{510} and [**1a**] in DMF, was significantly smaller than $k_b = 6.6 \times 10^7\ M^{-1}\ s^{-1}$ in HMPA (Figure 3). The ratio of k_b in DMF and in HMPA is 1:8. These results suggest that **1a**$^{\bullet-}$ decays mainly through neutralization with the solvent cation, $DMF(H^+)$ generated by initial radiolytic processes, that the formation of $(\mathbf{1a})_2^{\bullet-}$ is a minor process, and that a smaller k_b leads to a smaller yield of $(\mathbf{1a})_2^{\bullet-}$. The decay of the 450 nm band of **1a**$^{\bullet-}$ was analyzed by the second-order rate equation with the rate constant of the neutralization of **1a**$^{\bullet-}$ with $DMF(H^+)$, $k_n = 6.7 \times 10^{10}\ M^{-1}\ s^{-1}$ and $[DMF(H^+)]_0 = 2.8 \times 10^{-5}$ M. The 510 nm band of $(\mathbf{1a})_2^{\bullet-}$ decayed on a time scale of a few microseconds in DMF (Figure 1b). Because $(\mathbf{1a})_2^{\bullet-}$ did not decay on a 10 μs time scale, $k_n < 1 \times 10^9\ M^{-1}\ s^{-1}$ in HMPA was estimated. On the other hand, values of $k_n = 2.9 \times 10^{11}$ and $7.9 \times 10^9\ M^{-1}\ s^{-1}$ have been reported for the neutralization of **1a**$^{\bullet-}$ and an ion pair of **1a**$^{\bullet-}$/$(butyl)_4N^+$ in THF, respectively.[9c] These results suggest that $(\mathbf{1a})_2^{\bullet-}$ is the most stabilized in HMPA and more stabilized in DMF than in MTHF and that higher stabilization leads to a higher yield of $(\mathbf{1a})_2^{\bullet-}$. HMPA is a useful solvent in which high value of $G(e^-) = 2.3$ is obtained, and the organic radical anions generated are the most remarkably stabilized among many solvents.[4]

Formation of $\mathbf{2}_2^{\bullet-}$. The formation of a dimer radical anion of **2**$^{\bullet-}$ ($\mathbf{2}_2^{\bullet-}$) has been examined to determine the influence of the bonding character of $A^{\bullet-}$ on the formation of $A_2^{\bullet-}$. The transient absorption spectra with $\lambda_{max} = 480$ and >800 nm were

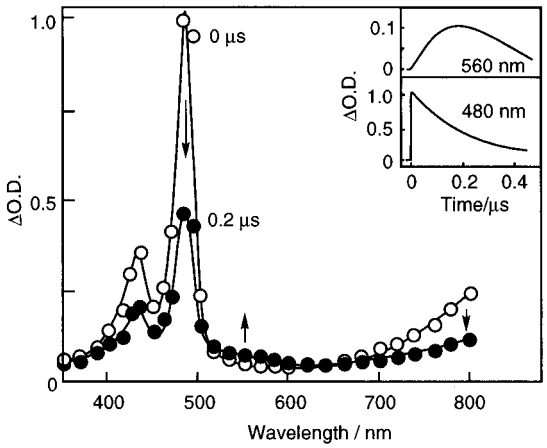

Figure 4. Transient absorption spectral changes during the pulse radiolysis of **2** with 1.0×10^{-2} M in degassed DMF solution at room temperature. Insets: time profiles of the transient absorptions at λ_{max} which are denoted in the figure.

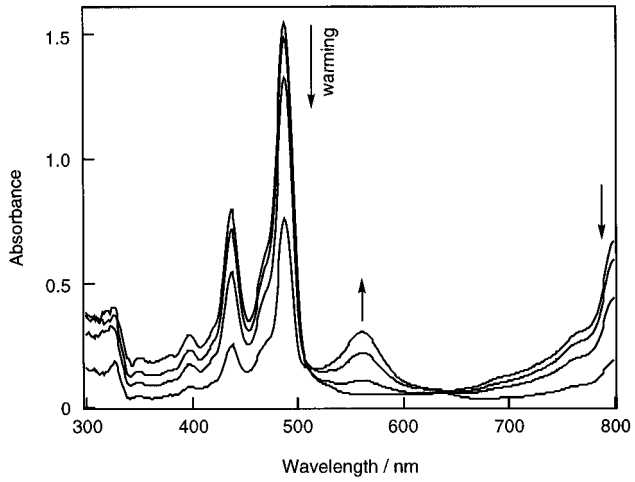

Figure 5. Absorption spectral changes of $\mathbf{2}^{\bullet-}$ upon warming below 100 K after γ-radiolysis of MTHF rigid matrix containing 2 with 5.0×10^{-3} M at 77 K.

SCHEME 2

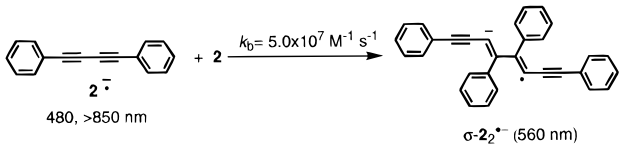

immediately observed after the electron pulse during the pulse radiolysis of **2** at 5.0×10^{-3} to 5.0×10^{-2} M in degassed DMF solution at room temperature (Figure 4). Because $[\mathbf{2}^{\bullet-}]_0$ is reasonably assumed to be equivalent to $[\mathbf{1a}^{\bullet-}]_0 = 2.8 \times 10^{-5}$ M,[27] $\epsilon_{480} = 8.9 \times 10^4$ M^{-1} cm^{-1} of $\mathbf{2}^{\bullet-}$ was calculated (Table 1) and found to be similar to $\epsilon_{480} = 1.1 \times 10^5$ M^{-1} cm^{-1} measured in THF.[9a] The value of $\lambda_{max} = 480$ nm of $\mathbf{2}^{\bullet-}$ shifted to a longer wavelength than $\lambda_{max} = 450$ nm for $\mathbf{1a}^{\bullet-}$. The transient absorption of $\mathbf{2}^{\bullet-}$ decayed with the formation of a band at $\lambda_{max} = 560$ nm. A similar absorption spectral change of $\mathbf{2}^{\bullet-}$ was observed after γ-radiolysis of **2** in an MTHF rigid matrix at 77 K (Figure 5). The absorption of $\mathbf{2}^{\bullet-}$ disappeared upon warming below 100 K, while a 560 nm band appeared. The results suggest that $\mathbf{2}^{\bullet-}$ dimerizes with **2** to $\mathbf{2}_2^{\bullet-}$ with the 560 nm band (Scheme 2).

The ratio of the ΔOD_{max} of $\mathbf{2}_2^{\bullet-}$ to the ΔOD_{max} of $\mathbf{2}^{\bullet-}$, equal to $[\mathbf{2}_2^{\bullet-}]_{max}/[\mathbf{2}^{\bullet-}]_0 = 0.10$, was approximately equivalent to $[(\mathbf{1a})_2^{\bullet-}]_{max}/[\mathbf{1a}^{\bullet-}]_0 = 0.09$. The result suggests that the yield of $\mathbf{2}_2^{\bullet-}$ is similar to that of $(\mathbf{1a})_2^{\bullet-}$. The pseudo-first-order rate constant of the formation of the 560 nm band (k_f^{560}) increased slightly with increasing [**2**]. The bimolecular rate constant of $k_b = 8.0 \times 10^6$ M^{-1} s^{-1} for $\mathbf{2}^{\bullet-}$, estimated from the relation of k_f^{560} and [**2**] in DMF (Supporting Information), was equivalent to $k_b = 8.2 \times 10^6$ M^{-1} s^{-1} for $\mathbf{1a}^{\bullet-}$. On the other hand, the decay profile of the 480 nm band was almost constant with $\tau_{1/2} = 230$ ns in the range of $[\mathbf{2}] = 5.0 \times 10^{-3}$ to 5.0×10^{-2} M. These results show that $\mathbf{2}^{\bullet-}$ decays mainly through neutralization with DMF(H^+) generated by initial radiolytic processes and that the formation of $\mathbf{2}_2^{\bullet-}$ is a minor process. The second-order rate constant of the neutralization of $\mathbf{2}^{\bullet-}$ was calculated to be $k_n = 7.3 \times 10^{10}$ M^{-1} s^{-1} from the decay of the 480 nm band and $[DMF(H^+)]_0 = 2.8 \times 10^{-5}$ M. The similar k_n values for $\mathbf{2}_2^{\bullet-}$ and $(\mathbf{1a})_2^{\bullet-}$ suggest similar stabilization of $\mathbf{2}_2^{\bullet-}$ and $(\mathbf{1a})_2^{\bullet-}$ in DMF.

From comparison of the results for $\mathbf{2}_2^{\bullet-}$ and $(\mathbf{1a})_2^{\bullet-}$ in DMF, it is suggested that the smaller k_b of $A^{\bullet-}$ leads to a smaller yield of $A_2^{\bullet-}$ and that the dimerization of $A^{\bullet-}$ is not much influenced by the bonding character of $A^{\bullet-}$ on the formation of $A_2^{\bullet-}$.

Formation of Intramolecular Dimer Radical Anions in $\mathbf{3}^{\bullet-}$. The formation of a dimer radical anion in $\mathbf{3}^{\bullet-}$ ($n = 2-6$) having two diphenylacetylene chromophores linked by a di-to-hexa methylene chain has been examined to elucidate the structure of σ-$(\mathbf{1a})_2^{\bullet-}$. It is essentially possible to form the dimer radical anions between two diphenylacetylene chromophores in an intramolecular and an intermolecular manner. The transient absorption spectra of $\mathbf{3}^{\bullet-}$ with $\lambda_{max} = 450$ and >840 nm were immediately observed after the electron pulse during the pulse radiolysis of **3** with 3.0×10^{-3} to 2.5×10^{-2} M in degassed HMPA solutions at room temperature (Figure 6). The $\Delta OD_{max} = 1.7-2.2$ and $\lambda_{max} = 440-450$ nm are similar to the $\Delta OD_{max} = 1.8$ and $\lambda_{max} = 450$ nm for $\mathbf{1a}^{\bullet-}$, respectively (Tables 1 and 2). Because $[\mathbf{3}^{\bullet-}]_0$ is reasonably assumed to be equivalent to $[\mathbf{1a}^{\bullet-}]_0 = 8.3 \times 10^{-5}$ M, $\epsilon_{max} = (5.1-8.1) \times 10^4$ M^{-1} cm^{-1} for $\mathbf{3}^{\bullet-}$ were calculated from ΔOD_{max} and $l = 0.4$ cm and were comparable to $\epsilon_{450} = 5.4 \times 10^4$ M^{-1} cm^{-1} for $\mathbf{1a}^{\bullet-}$ (Table 2). These results indicate that the radical anion is localized in one diphenylacetylene chromophore in $\mathbf{3}^{\bullet-}$. In other words, one diphenylacetylene chromophore changes to $\mathbf{1a}^{\bullet-}$ in $\mathbf{3}^{\bullet-}$ (Scheme 3).

The transient absorption of $\mathbf{3}^{\bullet-}$ decayed with the formation of a band at $\lambda_{max} = 510$ nm with isosbestic points at approximately 470 and 630 nm. The decay of the 450 and 800 nm bands and the formation of the 510 nm band were analyzed by the first-order rate equation with the first-order rate constants (k_m) which were almost constant for $\mathbf{3}^{\bullet-}$ ($n = 2-6$) in the range of $[\mathbf{3}] = 1.0 \times 10^{-3}$ to 2.5×10^{-2} M. No dependence of k_m on [**3**] was observed (Supporting Information). Because the 510 nm band is similar to that of σ-$(\mathbf{1a})_2^{\bullet-}$ from the dimerization of $\mathbf{1a}^{\bullet-}$ and **1a** (Figure 1a), it is assigned to the intramolecular dimer radical anions of $\mathbf{3}^{\bullet-}$ in which intramolecular σ-$(\mathbf{1a})_2^{\bullet-}$ is formed between $\mathbf{1a}^{\bullet-}$ and **1a**. k_m is the unimolecular rate constant of the formation of intramolecular $(\mathbf{1a})_2^{\bullet-}$, $k_m = (3.4-6.3) \times 10^5$ s^{-1} was calculated from the decay of the 450 and 800 nm bands and the formation of the 510 nm band in $\mathbf{3}^{\bullet-}$ (Table 2). The dimerization of $\mathbf{3}^{\bullet-}$ and **3** at $[\mathbf{3}] = 1.0 \times 10^{-3}$ to 2.5×10^{-2} M was not observed on a time scale of a few microseconds. The lack of the intermolecular dimerization seems to be attributed to the 4-$C_6H_4C{\equiv}CPh$ substituent of $\mathbf{3}^{\bullet-}$ and **3** at the 4-position because of the electronic and steric effects.

The ΔOD_{510} values of intramolecular $(\mathbf{1a})_2^{\bullet-}$ in $\mathbf{3}^{\bullet-}$ ($n = 2$, 3, 5, and 6) were much smaller in comparison, while that of intramolecular $(\mathbf{1a})_2^{\bullet-}$ in $\mathbf{3}^{\bullet-}$ ($n = 4$) was comparable to that of intermolecular $(\mathbf{1a})_2^{\bullet-}$. Therefore, the formation yield of

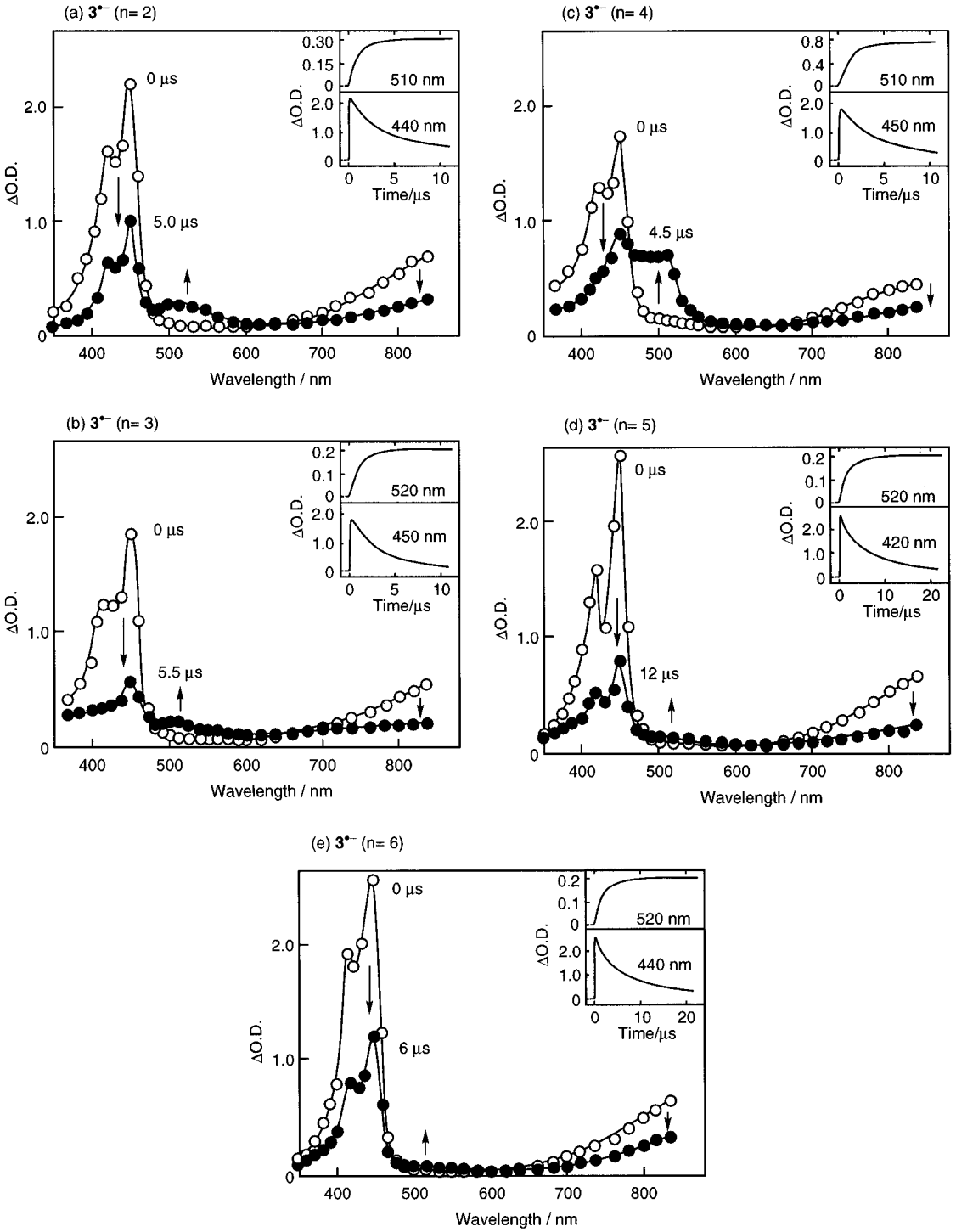

Figure 6. Transient absorption spectral changes during the pulse radiolysis of **3** with 1.0×10^{-2} M; $n = 2$ (a), $n = 3$ (b), $n = 4$ (c), $n = 5$ (d), and $n = 6$ (e) in degassed HMPA solutions at room temperature. Insets: time profiles of the transient absorptions at λ_{max} which are denoted in the figure.

SCHEME 3

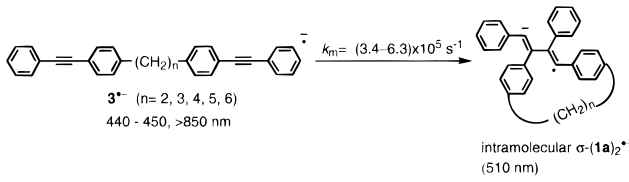

intramolecular $(\mathbf{1a})_2^{\bullet-}$ decreased with the existence of a methylene chain of $n = 2$, 3, 5, and 6. Because the yield for $\mathbf{3}^{\bullet-}$ ($n = 4$) was significantly high among $\mathbf{3}^{\bullet-}$ ($n = 2-6$) and comparable with that of intermolecular $(\mathbf{1a})_2^{\bullet-}$, the formation of intramolecular $(\mathbf{1a})_2^{\bullet-}$ occurs preferentially in $\mathbf{3}^{\bullet-}$ ($n = 4$).

TABLE 2: Intramolecular Dimerization of $\mathbf{3}^{\bullet-}$ in HMPA[a]

n of $(CH_2)_n$ in $\mathbf{3}^{\bullet-}$	λ_{max}/nm		ΔOD_{max}		$[(\mathbf{1a})_2^{\bullet-}]_{max}/[\mathbf{1a}^{\bullet-}]_0$	ϵ_{max}/ M^{-1} cm^{-1}	k_m of $(\mathbf{1a})_2^{\bullet-}/s^{-1}$
	$\mathbf{1a}^{\bullet-}$	$(\mathbf{1a})_2^{\bullet-}$	$\mathbf{1a}^{\bullet-}$	$(\mathbf{1a})_2^{\bullet-}$			
2	450	510	2.2	0.25	0.11	6.6×10^4	4.5×10^5
3	450	510	1.8	0.25	0.14	5.4×10^4	5.6×10^5
4	450	510	1.7	0.73	0.44	5.1×10^4	6.3×10^5
5	440	510	2.7	0.16	0.06	8.1×10^4	4.4×10^5
6	440	510	2.7	0.13	0.05	8.1×10^4	3.4×10^5

[a] $\mathbf{1a}^{\bullet-}$ and $(\mathbf{1a})_2^{\bullet-}$ denote the monomer and intramolecular dimer in $\mathbf{3}^{\bullet-}$, respectively. The unimolecular rate constant (k_m) of the intramolecular dimerization of $\mathbf{1a}^{\bullet-}$ and **1a** in $\mathbf{3}^{\bullet-}$ was calculated from the decay of 440−450 and 800 nm bands and the formation of the 510 nm band.

It is suggested that $n = 4$ make $\mathbf{3}^{\bullet-}$ flexible enough for an intramolecular $(\mathbf{1a})_2^{\bullet-}$ similar to intermolecular $(\mathbf{1a})_2^{\bullet-}$. It is known that intramolecular π-interaction between two π-chromophores B in the excited state exists significantly in $B-(CH_2)_3-B$ among intramolecular π-interaction model compounds $B-(CH_2)_n-B$ where two Bs are linked by a methylene chain $(CH_2)_n$. The rule of $n = 3$ is effective for the intramolecular π-interaction of $B-(CH_2)_n-B$ in the excited state[28] but not for that of intramolecular σ-$(\mathbf{1a})_2^{\bullet-}$ in $\mathbf{3}^{\bullet-}$ where $n = 4$ is effective.

Formation of $(\mathbf{1a})_2^{\bullet-}$ and $(\mathbf{1a})_2^{2-}$. $\mathbf{1a}^{\bullet-}/Na^+$ generated from the reduction by sodium metal has an absorption at $\lambda_{max} = 450$ nm[7,8] similar to $\mathbf{1a}^{\bullet-}$ generated during the pulse radiolysis and γ-radiolysis. $\mathbf{1a}^{\bullet-}/Na^+$ reacts with $\mathbf{1a}^{\bullet-}/Na^+$ to give $(\mathbf{1a})_2^{2-}/2Na^+$, but not with **1a**.[7,8] The absorption of $(\mathbf{1a})_2^{2-}/2Na^+$ has been observed on a time scale of a minute to an hour at room temperature with the usual absorption measurements. On the other hand, $\mathbf{1a}^{\bullet-}$ generated during the pulse radiolysis and γ-radiolysis reacts with **1a** at high [**1a**] to give $(\mathbf{1a})_2^{\bullet-}$ which was detected with transient absorption measurements on a time scale of a few tens of microseconds at room temperature. The difference will be discussed below with respect to $[\mathbf{1a}^{\bullet-}]_0$, the rate constants of the dimerization of $\mathbf{1a}^{\bullet-}$ with **1a** or $\mathbf{1a}^{\bullet-}$, and the stabilities or lifetimes of $(\mathbf{1a})_2^{\bullet-}$ and $(\mathbf{1a})_2^{2-}/2Na^+$.

First, it might be expected that the difference is due to the difference of $[\mathbf{1a}^{\bullet-}]_0$ in the reduction by sodium metal ($[\mathbf{1a}^{\bullet-}]_0 = 3.5 \times 10^{-3}$ to 7.3×10^{-2} M) and in the radiolyses ($[\mathbf{1a}^{\bullet-}]_0 = 8.3 \times 10^{-5}$ M). Because $(\mathbf{1a})_2^{\bullet-}$ is formed at $k_f = 3.3 \times 10^5$ to 2.6×10^6 s^{-1} depending on [**1a**] $= 5.0 \times 10^{-3}$ to 4.0×10^{-2} M, $\mathbf{1a}^{\bullet-}$ dimerizes with **1a** at $k_b = 7.3 \times 10^6$ to 6.6×10^7 M^{-1} s^{-1}. The bimolecular rate constant of the formation of $(\mathbf{1a})_2^{2-}$ has been reported to be 600−700 M^{-1} s^{-1} in THF at 273 K.[8] The rate constant is assumed to be the same in THF and HMPA; therefore, the apparent rate constants for the formation of $(\mathbf{1a})_2^{2-}$ are calculated to be $k_{app} = (5.0-5.8) \times 10^{-2}$ and 4.4−5.1 s^{-1} for $[\mathbf{1a}^{\bullet-}] = 8.3 \times 10^{-5}$ and 7.3×10^{-3} M, respectively. It is clearly suggested that the formation of $(\mathbf{1a})_2^{2-}$ cannot occur competitively with the formation of $(\mathbf{1a})_2^{\bullet-}$ on a time scale of a few tens of microseconds during the pulse radiolysis at room temperature.

Alternatively, stabilization of $(\mathbf{1a})_2^{2-}$ with the existence of Na^+ is suggested. $(\mathbf{1a})_2^{2-}$ is formed as an ion pair of $(\mathbf{1a})_2^{2-}/2Na^+$ from the dimerization of $\mathbf{1a}^{\bullet-}/Na^+$. Even though the rate constant of 600−700 M^{-1} s^{-1} is small, $(\mathbf{1a})_2^{2-}/2Na^+$ is sufficiently stable to be accumulated on a time scale of a minute to an hour. Such stabilization does not exist during the pulse radiolysis in which $\mathbf{1a}^{\bullet-}$ is generated as a free-radical ion.

Although the formation of $(ArH)_2^{\bullet-}$ has not been observed for most of ArH,[1−10] the dimerization of $A^{\bullet-}$ and A was detected in solution at room temperature and in a rigid matrix at 77 K in the present study. No direct evidence for the formation of π-$A_2^{\bullet-}$ suggests that $A^{\bullet-}$ is stabilized by the formation of σ-$A_2^{\bullet-}$ with a C−C bond between two sp carbons of $A^{\bullet-}$ and A and that the formation of σ-$A_2^{\bullet-}$ is responsible for the C−C triple bonds of $A^{\bullet-}$ and A. Questions on the lack of formation of π-$A_2^{\bullet-}$ and π-$(ArH)_2^{\bullet-}$ are still open for discussion.

Conclusions

Radical anions of aromatic acetylenes ($A^{\bullet-} = \mathbf{1}^{\bullet-}$ and $\mathbf{2}^{\bullet-}$) dimerize with the neutral molecule (A) to give σ-$A_2^{\bullet-}$ with a diene-type structure having one C−C bond between two sp carbons at $k_b = 7.3 \times 10^6$ to 6.6×10^7 M^{-1} s^{-1} at room temperature. The dimerization has also been observed upon warming of 77 K rigid matrices of $A^{\bullet-}$. The yield of the formation of intermolecular σ-$\mathbf{1}_2^{\bullet-}$ decreased with strong electronic substituents on one benzene ring ($\mathbf{1d}^{\bullet-}-\mathbf{1g}^{\bullet-}$). The yield of the formation of σ-$A_2^{\bullet-}$ was more stabilized in HMPA than in DMF and MTHF. The formation of the intramolecular σ-$(\mathbf{1a})_2^{\bullet-}$ occurs in the dimer model compounds $\mathbf{3}^{\bullet-}$, particularly with a tetramethylene chain ($n = 4$).

Acknowledgment. We thank Dr. Akito Ishida and Mr. Daizo Baba for their help in the experiments and the members of the Radiation Laboratory of ISIR, Osaka University, for running the linear accelerator. This work was partly defrayed by the Grants-in-Aid for Scientific Research (Nos. 07455341, 08240229), for Priority-Area-Research "Photoreaction Dynamics (No. 06239106) and "Quantum Tunneling" (No. 08240229) from the Ministry of Education, Science, Sports, and Culture of Japan.

Supporting Information Available: Properties of compounds prepared, transient absorption spectra and the time profiles of $\mathbf{1b}^{\bullet-}-\mathbf{1g}^{\bullet-}$ during the pulse radiolysis of **1b**−**1g** at 1.0×10^{-2} M in degassed HMPA solutions at room temperature, plots of the pseudo-first-order rate constant (k_f), the half-lifetime ($\tau_{1/2}$), or the first-order rate constant (k_m) calculated from the decay and formation of transient absorptions vs [**1c**], [**2**], or [**3** ($n = 4$)] during the pulse radiolyses of **1c**, **2**, and **3** ($n = 4$) in degassed HMPA solution at room temperature, respectively (7 pages). Ordering information is given on any current masthead page.

References and Notes

(1) (a) Hamill, W. H. In *Radical Ions*; Kaiser, E. T., Kevan, L., Eds.; Interscience: New York, 1968. (b) Tabata, Y., Ed. *CRC Handbook of Radiation Chemistry*; CRC Press: Boca Raton, FL, 1991; p 395−467.

(2) (a) Arai, S.; Dorfman, L. M. *J. Chem. Phys.* **1964**, *41*, 2190. (b) Arai, S.; Grev, D. A.; Dorfman, L. M. *J. Chem. Phys.* **1967**, *46*, 2537. (c) Arai, S.; Kira, A.; Imamura, M. *J. Phys. Chem.* **1977**, *81*, 110.

(3) (a) Shida, T.; Iwata, S. *J. Chem. Phys.* **1972**, *56*, 2858. (b) Shida, T.; Hamill, W. *J. Phys. Chem.* **1966**, *44*, 2369. (c) Shida, T. *Electronic Absorption Spectra of Radical Ions*; Elsevier: Amsterdam, 1988.

(4) Shaede, E. A.; Dorfman, L. M.; Flynn, G. F.; Walker, D. C. *Can. J. Chem.* **1973**, *51*, 3905.

(5) Cserhegyi, A.; Chaudhuri, J.; Franta, E.; Jagur-Grodzinski, J.; Szwarc, M. *J. Am. Chem. Soc.* **1967**, *89*, 7129.

(6) Wang, H. C.; Levin, G.; Szwarc, M. *J. Am. Chem. Soc.* **1977**, *99*, 2624.

(7) Dadley, D.; Evans, A. G. *J. Chem. Soc. (B)* **1967**, 418.

(8) Levin, G.; Jagur-Grodzinski, J.; Szwarc, M. *J. Am. Chem. Soc.* **1970**, *92*, 2268−2275.

(9) (a) Yamamoto, S.; Yamamoto, Y.; Hayashi, K. *Bull. Chem. Soc. Jpn.* **1991**, *64*, 346. (b) Aoyama, T.; Yamamoto, Y.; Hayashi, K. *J. Chem. Soc., Faraday Trans. 1* **1989**, *85*, 3353. (c) Yamamoto, Y.; Nishida, S.; Ma, X.-H.; Hayashi, K. *J. Phys. Chem.* **1986**, *90*, 1921.

(10) (a) Fujita, M.; Ishida, A.; Majima, T.; Takamuku, S. *J. Phys. Chem.* **1996**, *100*, 5382. (b) Majima, T.; Fukui, M.; Ishida, A.; Takamuku, S. *J. Phys. Chem.* **1996**, *100*, 8913.

(11) (a) Badger, B.; Brocklehurst, B. *Nature* **1968**, *219*, 263. (b) Badger B.; Brocklehurst, B. *Trans. Faraday Soc.* **1969**, *65*, 2588. (c) Badger, B.; Brocklehurst, B. *Trans. Faraday Soc.* **1969**, *65*, 2939. (d) Badger, B.; Brocklehurst, B.; Russel, R. D. *Chem. Phys. Lett.* **1967**, *1*, 122.

(12) Lewis, I. C.; Singer, L. S. *J. Chem. Phys.* **1965**, *43*, 2712.

(13) Ito, M. *J. Am. Chem. Soc.* **1971**, *93*, 4750.

(14) (a) Ichikawa, T.; Ludwig, P. K. *J. Am. Chem. Soc.* **1969**, *91*, 1024. (b) Ichikawa, T.; Ohta, N.; Kajioka, H. *J. Phys. Chem.* **1979**, *83*, 284.

(15) (a) Yoshida, H.; Noda, M.; Irie, M. *Polym. J.* **1971**, *2*, 359. (b) Hayashi, K.; Irie, M.; Lindenau, D.; Schnabel, W. *Europ. Polym. J.* **1977**, *13*, 925. (c) Hayashi, K.; Irie, M.; Lindenau, D.; Schnabel, W. *Radiat. Phys. Chem.* **1978**, *111*, 139. (d) Irie, S.; Hori, H.; Irie, M. *Macromolecules* **1980**, *13*, 1355. (e) Irie, S.; Irie, M. *Macromolecules* **1986**, *19*, 2182.

(16) (a) Kira, A.; Arai, S.; Imamura, M. *J. Chem. Phys.* **1971**, *54*, 4890. (b) Kira, A.; Arai, S.; Imamura, M. *J. Phys. Chem.* **1972**, *76*, 1119. (c) Arai, S.; Kira, A.; Imamura, M. *J. Chem. Phys.* **1972**, *56*, 1777. (d) Kira, A.; Imamura, M.; Shida, M. *J. Phys. Chem.* **1976**, *80*, 1445. (e) Kira, A.; Imamura, M. *J. Phys. Chem.* **1979**, *83*, 2267. (f) Egusa, S.; Arai, S.; Kira, A.; Imamura, M.; Tabata, Y. *Radiat. Phys. Chem.* **1977**, *9*, 419. (g) Egusa,

S.; Tabata, Y.; Arai, S.; Kira, A.; Imamura, M. *J. Polym. Sci., Polym. Chem. Ed.* **1978**, *16*, 729.

(17) (a) Rogers, M. A. J. *Chem. Phys. Lett.* **1971**, *9*, 107. (b) Rogers, M. A. J. *Trans. Faraday Soc. 1* **1972**, *68*, 1278.

(18) Brede, O.; Bos, J.; Helmstreit, W.; Mehnert, R. *Radiat. Phys. Chem.* **1982**, *19*, 1.

(19) (a) Yamamoto, Y.; Chikai, Y.; Hayashi, K. *Bull. Chem. Soc. Jpn.* **1985**, *58*, 3369. (b) Chikai, Y.; Yamamoto, Y.; Hayashi, K. *Bull. Chem. Soc. Jpn.* **1988**, *61*, 2281.

(20) (a) Akaba, R.; Sakuragi, H.; Tokumaru, K. *Chem. Phys. Lett.* **1990**, *174*, 80. (b) Kuriyama, Y.; Sakuragi, H.; Tokumaru, K.; Yoshida, Y.; Tagawa, S. *Bull. Chem. Soc. Jpn.* **1993**, *66*, 1852.

(21) (a) Tujii, Y.; Tsuchida, A.; Yamamoto, M. *Macromolecules* **1990**, *23*, 4019. (b) Tujii, Y.; Tsuchida, A.; Ito, S.; Onogi, Y.; Yamamoto, M. *Macromolecules* **1991**, *24*, 4061. (c) Tsuchida, A.; Tujii, Y.; Ohoka, M.; Yamamoto, M. *J. Phys. Chem.* **1991**, *95*, 5797. (d) Tujii, Y.; Tsuchida, A.; Yamamoto, M.; Momose, T.; Shida, T. *J. Phys. Chem.* **1991**, *95*, 8635. (e) Tsuchida, A.; Yamamoto, M. *J. Photochem. Photobiol. A: Chem.* **1992**, *65*, 53. (f) Tsuchida, A.; Ikawa, T.; Toie, T.; Yamamoto, M. *J. Phys. Chem.* **1995**, *99*, 8196. (g) Tsuchida, A.; Ikawa, T.; Yamamoto, M.; Ishida, A.; Takamuku, S. *J. Phys. Chem.* **1995**, *99*, 14793.

(22) (a) Tojo, S.; Morishima, K.; Ishida, A.; Majima, T.; Takamuku, S. *Bull. Chem. Soc. Jpn.* **1995**, *68*, 958. (b) Tojo, S.; Morishima, K.; Ishida, A.; Majima, T.; Takamuku, S. *J. Org. Chem.* **1995**, *60*, 4684. (c) Majima, T.; Tojo, S.; Ishida, A.; Takamuku, S. *J. Phys. Chem.* **1996**, *100*, 13615. (d) Majima, T.; Tojo, S.; Ishida, A.; Takamuku, S. *J. Org. Chem.* **1996**, *61*, 7793.

(23) Stephens, R. D.; Castro, C. E. *J. Org. Chem.* **1963**, *28*, 3313.

(24) Since the values of $\epsilon_{450} = (2.7-5.6) \times 10^4$ M^{-1} cm^{-1} of **1a**$^{\bullet-}$ measured in THF, MTHF, and HMPA are in the same order of magnitude, the value of $\epsilon_{450} = 5.4 \times 10^4$ M^{-1} cm^{-1} in HMPA[8] was taken for the calculation.

(25) Wawzonek, S.; Wearring, D. *J. Am. Chem. Soc.* **1959**, *81*, 2067.

(26) Sioda, R. E.; Cowan, D. O.; Koski, W. S. *J. Am. Chem. Soc.* **1967**, *89*, 7356.

(27) The value of $\epsilon_{449} = 5.6 \times 10^4$ M^{-1} cm^{-1} of **1a**$^{\bullet-}$ in THF has been reported based on $G(e^-) = 1.2$ in THF[9c] during the pulse radiolysis of **1a**.[9a]

(28) Hirayama, F. *J. Chem. Phys.* **1965**, *42*, 3163.